Journal of Thermal Analysis and Calorimetry (2018) 132:263–273
https://doi.org/10.1007/s10973-017-6906-z

Gas–condensed phase flame-retardant mechanisms of tris(3-nitrophenyl) phosphine/triphenyl phosphate/ABS

Hang Luo[1] · Feng Zhou[1] · Yunyun Yang[1] · Xilei Cao[1] · Xufu Cai[1]

Received: 16 July 2017 / Accepted: 5 December 2017 / Published online: 13 December 2017

Abstract
Tris(3-nitrophenyl) phosphine (NPPh3), a flame retardant containing phosphorus and nitro group, is synthesized. And a novel flame retardant loading with NPPh3 and triphenyl phosphate (TPP) is prepared to flame-retardant acrylonitrile–butadiene–styrene (ABS). The effects of NPPh3 and TPP on the flammability of ABS are studied by various methods. The flame retardation of ABS/NPPh3/TPP composite is characterized by limiting oxygen index method and vertical and horizontal burning tests (UL-94). Compared with the systems with ABS/NPPh3 and ABS/TPP alone, ABS/NPPh3/TPP obtains a higher limiting oxygen index. Additionally, the flame-retardant effect of ABS/NPPh3/TPP in condensed phase is studied by thermogravimetric analysis (TG), scanning electron microscopy, and Fourier transform infrared spectroscopy (FTIR). The gases evolved during thermal degradation process in nitrogen are studied by means of thermogravimetry coupled with Fourier transform infrared spectroscopy (TG-FTIR). The results show that ABS/NPPh3/TPP exerts gas-condensed phase flame-retardant effect.

Keywords Flame retardant · ABS · NPPh3 · TPP · Synergistic effect

Introduction

Acrylonitrile–butadiene–styrene (ABS) is a kind of copolymer formed with acrylonitrile, butadiene, and styrene [1], which has been applied widely in consumer electronics [2], automobile parts [3], and 3D printing [4], owing to its attractive properties such as easy processing, good mechanical strength, chemical resistance, and shining surface [5]. However, flammability is one of the major drawbacks of ABS, which restricts their further applications for safety consideration [6]. Therefore, for the sake of meeting application requirements, it is significant to improve the flame retardancy of ABS.

Bromine-containing compounds, such as decabromodiphenyl oxide (DBDPO) and tetrabromobisphenol A (TBBPA), are very effective and show a good ratio of property to price in flame retardancy of ABS resin [7]. However, they are subjected to strict regulation in many fields because of releasing toxic gases in the process of combustion [8]. Therefore, from the viewpoint of environmental protection, halogen-free ABS resin has attracted increasing attention.

Organic phosphorus compounds are important class of flame retardants with high retardant efficiency [9]. When the thermal degradation occurs, polyphosphoric acid will be produced, which esterifies and dehydrates the pyrolyzing polymer. Meanwhile, the polymeric phosphoric acids inhibit further pyrolysis by forming a carbon layer [10]. Among these types of flame retardants, triphenyl phosphate (TPP) is widely used to react with ABS to prepare flame-retardant thermosets owing to its good fire-retarding performance [11]. However, without co-additive, ABS modified with TPP cannot show high thermal stability. Studies about TPP have focused on the additives constructed by several functional groups such as silicon [12], epoxy group [13], and hydroxyl group [14]. These additives can confirm synergistic flame-retardant effect with TPP and thus endow matrix by high flame retardancy. Additives containing nitro group can exert flame-retardant effect [15]; however, whether a combination of nitro compound with TPP will result in enhanced flame retardancy is unknown.

✉ Xufu Cai
caixf2008@scu.edu.cn

[1] College of Polymer Science and Materials, Sichuan University, Chengdu 610065, China

In this work, nitro compound, that is tris(3-nitrophenyl) phosphine (NPPh3), is prepared in our laboratory. The TPP and NPPh3 are used as flame retardants for ABS, with the purpose of studying synergistic effect of TPP and compound containing nitro group influence on the flame retardancy efficiency for ABS. The thermal degradation behavior and flame-retardant effect are investigated by limiting oxygen index (LOI) method, vertical and horizontal burning tests (UL-94), thermogravimetric analysis (TG), scanning electron microscopy (SEM), Fourier transform infrared spectroscopy (FTIR), and thermogravimetry coupled with Fourier transform infrared spectroscopy (TG-FTIR).

Experimental

Materials

Acrylonitrile–butadiene–styrene copolymer (0215A) was supplied by Jilin Petrochemical Company Limited. TPP, triphenylphosphine (PPh3), sodium bicarbonate, sulfuric acid, and nitric acid were purchased from Chengdu Kelong Chemical Reagent Factory.

Synthesis of tris(3-nitrophenyl) phosphine

NPPh3 was synthesized through the nitration reaction of PPh3, using the already reported method [16]. PPh3 (2.62 g, 0.01 mol) and sulfuric acid (20 g, 0.2 mol) were added to a 100-ml three-necked round-bottom flask equipped with a thermometer, a stirrer, and a constant-pressure dropping funnel. PPh3 was dissolved in sulfuric acid with stirring at room temperature. After that, the temperature of the mixed system was reduced to below 10 °C with an ice-salt bath and the mixed solution of sulfuric acid (30 g, 0.3 mol) and nitric acid (6 g, 0.06 mol) was slowly added dropwise for 30 min [17]. Then the reaction mixture was warmed to room temperature and then stirred for 6 h. The product was precipitated by pouring the reaction mixture over an excess of ice-cold water, neutralizing with saturated sodium bicarbonate solution, washing with water, and filtering. Finally, 3.9 g light yellow product was obtained with the yield of 89%.

Sample preparation

ABS resin with different NPPh3 and TPP contents was mixed in a Haake plastic mixer at 175 °C and 60 rpm for 5 min. The mixed samples were transferred to a mold and preheated at 170 °C for 8 min. Then they were pressed at 10 MPa and successively cooled to room temperature, and the pressure was maintained to obtain the composite sheets for further measurements.

Characterizations

Fourier transform infrared spectra

Fourier transform infrared spectra (FTIR) were obtained with a Nicolet Magna-FTIR 560 spectrometer (Nicolet Instrument Co., the USA). The FTIR tests were carried out under air atmosphere and in the wavenumber range from 500 to 4000 cm^{-1}. The sample was thoroughly mixed with KBr and then pressed into pellets.

Nuclear magnetic resonance

^{1}HNMR (600 MHz) spectrum was recorded on a FT-80A NMR using $CDCl_3$ as the solvent and internal standard.

Thermogravimetric analysis

Thermogravimetric analysis (TG) was performed on a Netzsch TG209 F1 at a heating rate of 10 °C min^{-1}. Five milligrams of the sample was examined under air and nitrogen atmosphere at a flowing rate of 60 mL min^{-1} at temperature from 30 to 800 °C.

Limiting oxygen index method

The limiting oxygen index (LOI) method data of all samples were obtained on an oxygen index instrument (XYC-75) produced by Chengde Jinjian Analysis Instrument Factory according to ASTMD 2863-08 standard with a specimen dimension of 130 × 6.5 × 3.2 mm^3 at room temperature.

Vertical and horizontal burning tests

Vertical and horizontal burning tests (UL-94) were carried out by a CZF-2 instrument (Jiangning Analysis Instrument Company, China) with a sample dimension of 125 × 12.5 × 3 mm^3 according to UL-94 ASTMD 635 standard at room temperature.

Scanning electron microscopy

Scanning electron microscopy (SEM) analysis was used to study the morphologies of residues obtained from combustion by UL-94 using a FEI Quanta-250 SEM.

Thermogravimetric analysis/infrared spectrometry

Thermogravimetric analysis/infrared spectrometry (TG-FTIR) were carried out on a Mettler Toledo TG/DSC 1 STAR^{e} System thermogravimeter coupled with a Nicolet iS10 FTIR spectrophotometer at a linear heating rate of 20 °C min^{-1} under nitrogen within 50–800 °C (Schemes 1 and 2).

Results and discussion

Characterization of NPPh3

In order to confirm the molecular structure of NPPh3, FTIR and ^{1}HNMR are carried out. Figure 1 is the FTIR spectrum of NPPh3. The absorption peaks at 3100–3000 cm^{-1} belong to benzene ring. The absorptions at 1525 and 1346 cm^{-1} are assigned to NO_2. The peak at 1469 cm^{-1} is associated with the vibrations of P-Ph. The peaks at 879, 733, and 674 cm^{-1} indicate that the product is 1,3-substituted on the phenyl ring. The ^{1}HNMR spectra of NPPh3 are shown in Fig. 2: 8.52–8.55 ppm (a), 8.46–8.52 ppm (b), 8.15–8.24 ppm (c), 7.95–7.90 ppm (d). All these characteristics indeed match the NPPh3 structure. The information above confirms that the target product is synthesized successfully.

Synergistic effect

In order to investigate the synergistic effect between NPPh3 and TPP, the thermal degradation behavior of NPPh3/TPP is studied by thermogravimetric analysis. Figure 3 shows the TG curves of NPPh3, TPP, and NPPh3/TPP (2:3) systems. The theoretical curve is calculated based upon the mass percentage of the ingredient. The formula is as follows:

$$Y_{\mathrm{cal}} = \mathrm{mass}_{\mathrm{NPPh3}}\% \times Y_{\mathrm{NPPh3exp}} + \mathrm{mass}_{\mathrm{TPP}}\% \times Y_{\mathrm{TPPexp}},$$

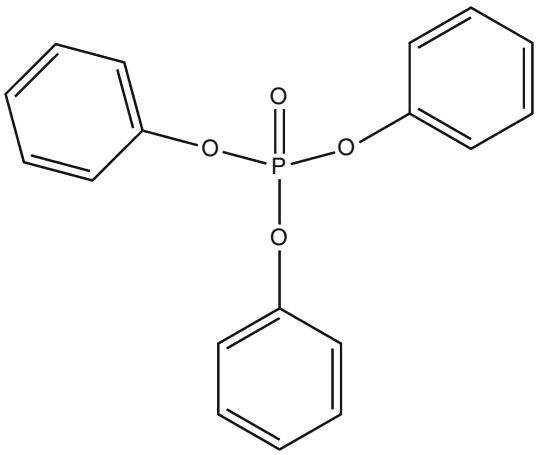

Scheme 1 Structure of triphenyl phosphate (TPP)

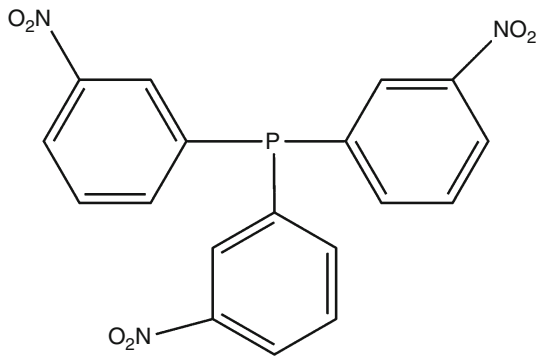

Scheme 2 Structure of tris(3-nitrophenyl) phosphine (NPPh3)

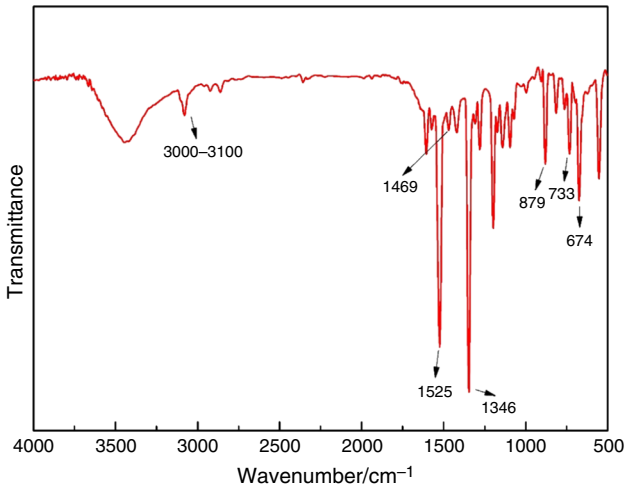

Fig. 1 FTIR spectrum of NPPh3

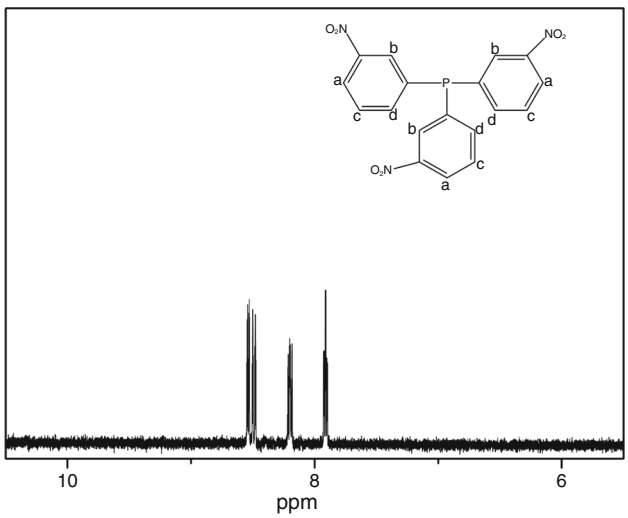

Fig. 2 1H-NMR spectrum of NPPh3

where mass% refers to the corresponding proportion of ingredients; Y_{cal} is the theoretical value of carbon residue; and Y_{exp} is the actual amount of carbon residue.

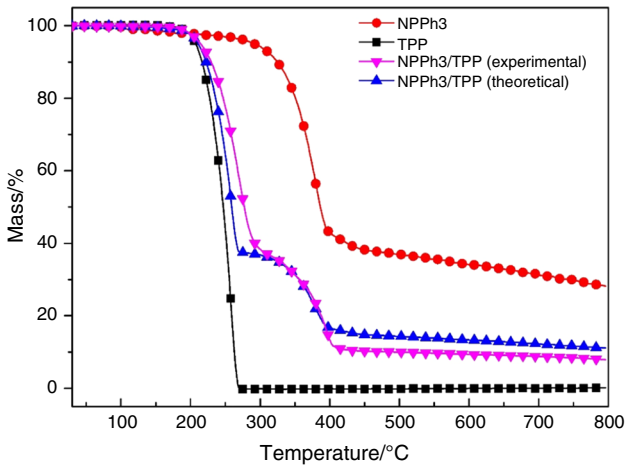

Fig. 3 Experimental and theoretical TG curves of NPPh3/DOPO (mass ratio = 2:3) under nitrogen

As shown in Fig. 3, NPPh3 is thermally stable below 290 °C, its thermal degradation occurs through one step, and its char residue at 800 °C is 28.16%. Comparatively, the degradation process of TPP, which also exhibits one step from 190 to 270 °C, leaves 0% charred residue under the same condition. When NPPh3 is combined with TPP, an obvious difference between experimental and theoretical is observed. Compared with theoretical curve, experimental curve slows down the mass loss of NPPh3/TPP system at first. This means a complicated reaction between NPPh3 and TPP happens. When the temperature exceeds 390 °C, theoretical char residual is higher than the experimental one. It is probably because NPPh3/TPP turns into low molar mass volatiles at high temperature.

Flame retardancy

The limiting oxygen index, i.e., the lowest volume concentration of oxygen sustaining the burning of materials in an oxygen–nitrogen flowing mixture, is an indicator to evaluate the ease of extinguishment of polymeric materials in the same atmosphere [18, 19]. Table 1 gives the LOI value and UL-94 results of ABS and flame-retardant ABS with a total loading of the NPPh3 and TPP additives of 20 mass%. It can be seen that the pure ABS is highly combustible with its LOI value only 18%. It is classified as no rating (NR) in the vertical burning test and FH-3 in the horizontal burning test. However, when the addition of TPP is 20 mass%, LOI value of the ABS/TPP system increases to 21% and FH-1 rating during horizontal burning test is reached. Table 1 also shows that when TPP is mixed with NPPh3, and then added to ABS, LOI value of ABS/NPPh3/TPP systems changes with the ratio of NPPh3 to TPP. These values increase with an increase in the ratio of NPPh3 to TPP and then decrease with a further increase in the ratio. When the mass ratio of NPPh3 to TPP is 2:3, that is, NPPh3 is 8 mass% and TPP is 12 mass%, the ABS/NPPh3/TPP shows the best flame retardancy with its LOI value reaching the maximum of 24%. It demonstrates that a suitable ratio of NPPh3 to TPP would bring synergistic effect to ABS and impose a better flame-retardant property on ABS.

Table 2 shows the influence of NPPh3/TPP addition on flame retardancy of ABS/NPPh3/TPP system, setting the ratio of NPPh3 to TPP as 2:3. It is found that LOI values of the ABS/NPPh3/TPP system increase with the increase in NPPh3/TPP loading. When the addition of NPPh3/TPP is 35 mass%, LOI value of ABS/NPPh3/TPP system is 25%, and UL-94 V-1 and FH-1 ratings are passed.

Analysis of flame-retardant mechanism in condensed phase

Thermal analysis

TG is one of the effective tools to evaluate thermal stability and thermal decomposition behaviors of various polymers [20]. Figure 4 shows the thermogravimetric and differential thermogravimetric curves of the ABS, ABS/NPPh3, ABS/TPP, and ABS/NPPh3/TPP-2 systems under N_2 atmosphere, and the corresponding $T_{5\%}$, R_{peak}, T_{max}, and Y_c are summarized in Table 3.

The thermal degradation of ABS occurs in a single step between 393.4 ($T_{5\%}$) and 500 °C with a maximum degradation rate at 428.3 °C (T_{max}), and its residual char at 800 °C is 4.95%, which means ABS shows poor charring ability itself. With the incorporation of NPPh3, the value of $T_{5\%}$ is 323.9 °C and its thermal degradation occurs in two steps. The decomposition temperature in the first step ranges from 270 to 330 °C, the second step is between 330 and 540 °C, and its main pyrolysis peaks appear at 314.5 and 422.3 °C, respectively. It can be seen that NPPh3 causes the early decomposition of ABS at a lower temperature, which can be attributed to the low bond energy of P–C [21]. Furthermore, the addition of NPPh3 improves the char formation of ABS and enhances the thermal stability of the polymer. Although with the addition of TPP, ABS/TPP shows a lower initial decomposition temperature (266.6 °C) too, it does not promote the formation of residue as NPPh3 does. (Y_c at 800 °C is 5.39%) This may be due to the volatilization of TPP at a low temperature. And this implies that TPP exerts more effect in gaseous phase and therefore relatively less effect in condensed phase. So, for ABS/TPP, the thermal degradation shows two peaks at 296.9 and 429.6 °C. The T_{1max} is due to the low volatile temperature of TPP, and the T_{2max} is consistent with that of ABS. When NPPh3 and TPP are incorporated into ABS in a certain ratio, ABS/NPPh3/TPP-2 exhibits a two-stage decomposition process. The initial thermal decomposition

Table 1 Flame retardancy of ABS composites

Samples	Composition/mass%				LOI/%	UL-94	
	ABS	NPPh3	TPP	NPPh3:TPP		Vertical burning rating	Horizontal burning rating
ABS	100	–	–	–	18	NR	FH-3
ABS/NPPh3	80	20	–	–	20.5	NR	FH-1
ABS/TPP	80	–	20	–	21	NR	FH-1
ABS/NPPh3/TPP-1	80	5	15	1:3	22	NR	FH-1
ABS/NPPh3/TPP-2	80	8	12	2:3	24	NR	FH-1
ABS/NPPh3/TPP-3	80	10	10	1:1	23.5	NR	FH-1
ABS/NPPh3/TPP-4	80	12	8	3:2	22.5	NR	FH-1
ABS/NPPh3/TPP-5	80	15	5	3:1	22	NR	FH-1

Table 2 Flame retardancy of ABS composites (NPPh3:TPP = 2:3)

Samples	Composition/mass%				LOI/%	UL-94	
	ABS	NPPh3	TPP	NPPh3:TPP		Vertical burning rating	Horizontal burning rating
ABS/NPPh3/TPP-2	80	8	12	2:3	24	NR	FH-1
ABS/NPPh3/TPP-6	75	10	15	2:3	24.5	NR	FH-1
ABS/NPPh3/TPP-7	70	12	18	2:3	24.8	NR	FH-1
ABS/NPPh3/TPP-8	65	14	21	2:3	25	V-1	FH-1

occurs between 200 and 340 °C; the second stage is from 340 to 540 °C. The initial decomposition temperature of ABS/NPPh3/TPP-2 is higher than those of ABS/TPP and lower than those of ABS/NPPh3. The residues yield of systems is in the order of ABS/NPPh3 > ABS/NPPh3/TPP-2 > ABS/TPP.

Pyrolysis process in air is similar to combustion condition [22]. The thermal degradation behavior of the various samples in air atmosphere is shown in Fig. 5, and the corresponding $T_{5\%}$, $R_{1\text{peak}}$, $T_{1\text{max}}$, and Y_c are summarized in Table 4.

As can be seen, compared with only one decomposition stage that takes place in nitrogen atmosphere, ABS experiences two stages of degradation process which occur at the temperatures of 340–470 °C and 520–620 °C in an air atmosphere, and the largest thermal degradation peaks appear at 428.9 and 570.2 °C. The first thermal degradation is assumed as the thermal degradation of the polymer network, and the second degradation is due to the char formed in the first stage that shows unstable thermal stability [23]. When the temperature reaches 378.4 °C, initial decomposition occurs, and the char residue yield of ABS is 10.89% at 500 °C and 5.04% at 800 °C.

Figure 5 shows that the degradation of ABS/NPPh3, ABS/TPP, and ABS/NPPh3/TPP-2 can be divided into three stages. It may be remarked that the first stage is the thermal degradation of the flame retardant; the second stage is mainly the degradation of ABS; and the third stage is the process of cross-linking, carbonization, and further taking off the small molecules until a stable carbonization structure is formed. With the respective addition of NPPh3 and TPP, there is a decrease in initial decomposition temperature, which is 326.9 and 256.3 °C. It is evident that TPP changes $T_{5\%}$ more drastically. What needs to be pointed out is that the $R_{2\text{peak}}$ of ABS/NPPh3 and ABS/TPP are lower than that of pure ABS, which demonstrates that NPPh3 and TPP help to moderate the degradation of ABS. When the temperature reaches 500 °C, the char residue of ABS/NPPh3 is 32.85% (three times of ABS), much higher than the value of ABS/TPP (11.60%). However, when the temperature reaches 800 °C, the char residue of ABS/NPPh3 is lower compared with ABS/TPP. Table 4 shows that $R_{3\text{peak}}$ of ABS/NPPh3 and ABS/TPP are 2.78% °C^{-1} and 1.05% °C^{-1}, respectively. This implies that the decomposition of char moiety of ABS/NPPh3 is stronger than that of ABS/TPP, which leads to the result above.

For ABS/NPPh3/TPP-2, the value of $T_{5\%}$, $R_{2\text{peak}}$, $T_{2\text{max}}$, $R_{3\text{peak}}$, $T_{3\text{max}}$, and Y_c at 500 °C is between that of ABS/NPPh3 and ABS/TPP. However, $R_{1\text{peak}}$ and $T_{1\text{max}}$ of ABS/NPPh3/TPP-2 are higher than the other two systems. It is

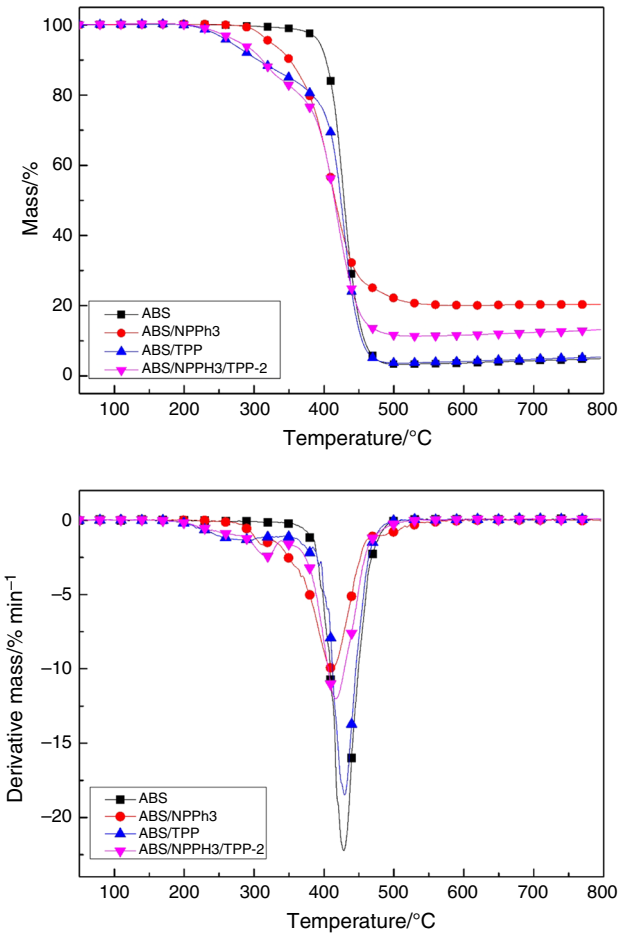

Fig. 4 TG and DTG curves for ABS and flame-retardant systems under pure nitrogen

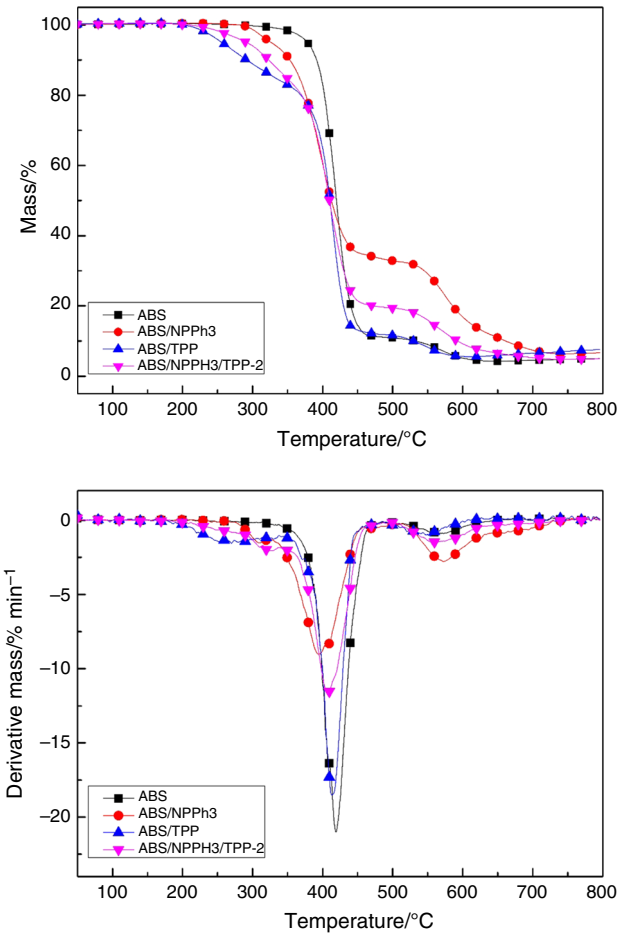

Fig. 5 TG and DTG curves for ABS and flame-retardant systems under air atmosphere

Table 3 TG and DTG data of different systems under N_2 atmosphere at a heating rate of 10 °C min^{-1}

Sample	$T_{5\%}$/ °C	R_{1peak}/% °C^{-1}	T_{1max}/ °C	R_{2peak}/% °C^{-1}	T_{2max}/ °C	Y_c at 800 °C/%
ABS	393.4	–	–	22.24	428.3	4.95
ABS/NPPh3	323.9	1.68	314.5	9.99	411.2	20.33
ABS/TPP	266.6	1.34	296.9	18.49	429.6	5.39
ABS/NPPh3/TPP-2	279.5	2.42	318.7	12.01	417.3	13.17

$T_{5\%}$ the temperature of 5% loss decomposition (set $T_{5\%}$ as initial decomposition temperature), T_{1max} and T_{2max} the temperatures of the first and second decomposition peaks, R_{1peak} and R_{2peak} the decomposition speeds at the first and second decomposition peaks, Y_c the char residues at 800 °C

the synergistic effect of NPPh3 and TPP which makes their decomposition in the first stage intensify. And it also leads to the relatively low value of Y_c at 800 °C.

Morphological study of the char residues

To explore the flame-retardant charring mechanism further, we investigate the residues of char after UL-94 by SEM. Figure 6a shows the residue SEM images of ABS, ABS/NPPh3, ABS/TPP, and ABS/NPPh3/TPP-2. We find that the charring layer, for pure ABS, is loose and rugged, which is related to bad flame-retardant performance. The residue of ABS/NPPh3 sample in Fig. 6b presents a continuous and smooth surface. From the results of TG, NPPh3 can effectively promote the formation of char residue. This tight char surface endows the materials with much high LOI. The residue of ABS/TPP sample in Fig. 6c is expansionary but porous, which might be formed because of permeation of gases resulting from decomposition of TPP. The char surface of ABS with both NPPh3 and TPP,

Table 4 TG and DTG data of different systems under air atmosphere at a heating rate of 10 °C min^{-1}

Sample	$T_{5\%}$/°C	R_{1peak}/% °C^{-1}	T_{1max}/ °C	R_{2peak}/% °C^{-1}	T_{2max}/ °C	R_{3peak}/% °C^{-1}	T_{3max}/ °C	Y_c/%	
								500 °C	800 °C
ABS	378.4	–	–	21.01	418.9	0.89	570.2	10.89	5.04
ABS/NPPh3	326.9	1.52	309.9	9.03	394.2	2.78	572.7	32.85	6.72
ABS/TPP	256.3	1.54	269.9	18.50	412.9	1.05	552.9	11.60	7.67
ABS/NPPh3/TPP-2	291.6	2.07	323.2	11.65	407	1.47	556.4	19.40	4.94

T_{3max} the temperature of the third decomposition peak; R_{3peak} the decomposition speed at the third decomposition peak

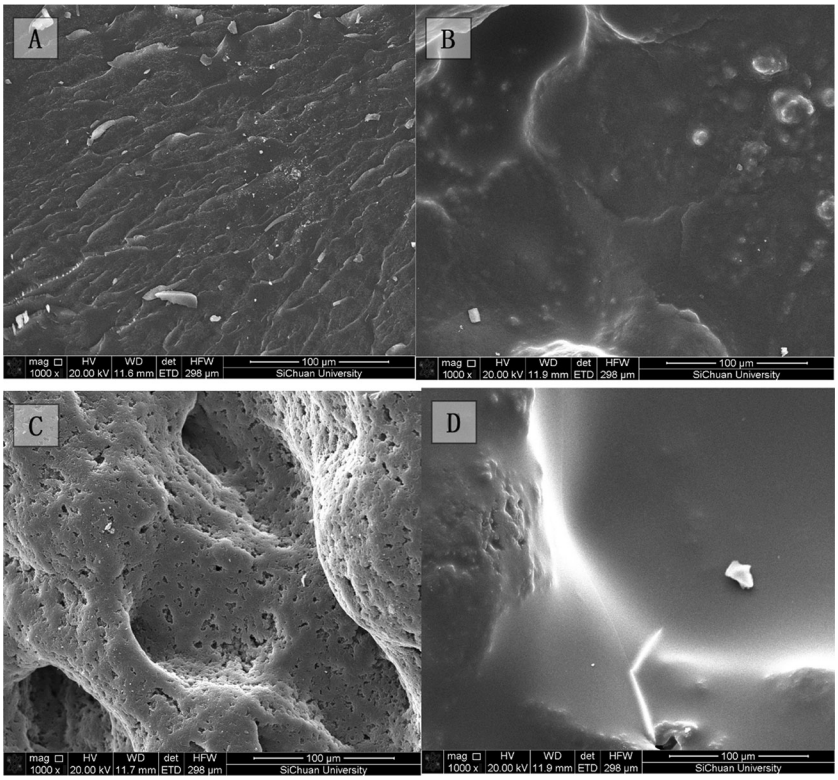

Fig. 6 SEM photographs of the residues from UL-94. **a** ABS, **b** ABS/NPPh3, **c** ABS/TPP, **d** ABS/NPPh3/TPP-2

illustrated in Fig. 6d, combines the characteristics of ABS/NPPh3 and ABS/TPP. However, the residue of ABS/NPPh3/TPP-2 is more smooth and tight than that of ABS/NPPh3. Meanwhile, the char layer for ABS/NPPh3/TPP-2 has less number of holes compared with ABS/TPP.

In order to understand the formation of condensed phase, the combustion residues of ABS, ABS/NPPh3, ABS/TPP, and ABS/NPPh3/TPP-2 collected after UL-94 are investigated by FTIR, and the FTIR spectra are shown in Fig. 7. It can be seen that peaks at 3434, 3026, 2922, 2853, 2360, 2236, 1628, 1493, and 1452 cm^{-1} are the absorptions of ABS. The broad peaks around 3434 cm^{-1} can be assigned to the stretching mode of O–H. The absorbance peaks at 3026, 1628, and 1493 cm^{-1} are attributed to aromatic compounds [24]. The bands at 2922 and 2853 cm^{-1} correspond to C–H. The peaks at 2360 and 2236 cm^{-1} are the characteristic vibration of C≡N. And the absorbance peak at 1452 cm^{-1} is assigned to methylene. It is evident that new absorbance peaks at 1594, 1304, 1275, 1169, and 1027 cm^{-1} appear in the FTIR spectrograms of ABS/NPPh3 and ABS/NPPh3/TPP-2. The absorption bands at 1508 and 1300 cm^{-1} demonstrate the existence of N–O bond in the char residue, which indicate the nitro group did not completely decompose after burning. It is necessary to point out that peaks at 1275 cm^{-1} and at 1169 and 1027 cm^{-1} are also observed in the spectrums of ABS/NPPh3 and ABS/NPPh3/TPP-2. These may be attributed to the P=O and P–O, respectively, suggesting that the char layer structure contains polyphosphoric acid [25]. The FTIR spectrograms of ABS and ABS/

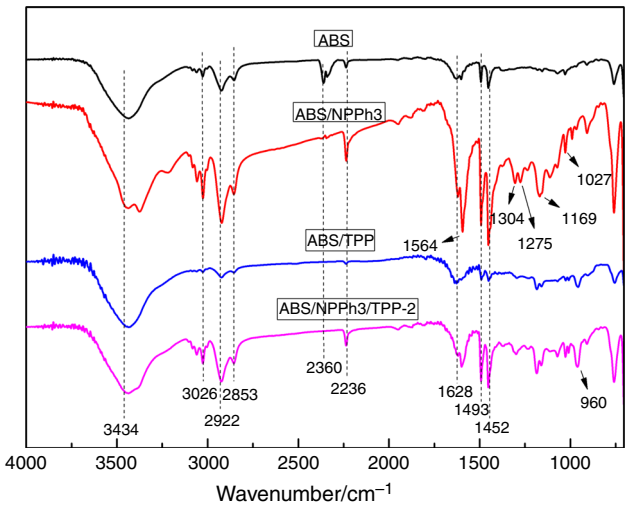

Fig. 7 FTIR spectra of the residue char of ABS, ABS/NPPh3, ABS/TPP, and ABS/NPPh3/TPP-2 after UL-94

TPP are almost same. These may be due to the TPP, which volatilizes in the combustion process. Absorbance peak of ABS/NPPh3/TPP-2 at 960 cm^{-1} indicates the existence of P–O–Ph structure, which is stronger than ABS/TPP and can be attributed to TPP, proving that the mixture of TPP and NPPh3 suppresses the evaporation of TPP due to the interaction of TPP and NPPh3.

Analysis of flame-retardant mechanism in gaseous phase

The TG-FTIR is used to analyze the gas products formed during the thermal degradation. In order to further explore the thermal degradation mechanism, the TG-FTIR spectra of ABS and ABS/NPPh3/TPP-2 are detected in a nitrogen atmosphere. Their FTIR spectra of the volatilized products at a series of temperatures and 3D TG-FTIR spectra of the pyrolysis products at a heating rate of 20 °C min^{-1} in nitrogen atmosphere are shown in Figs. 8 and 9. Peaks at 3600–3800, 3075, 3028, 2937, 1820, 1629, 1494, 1444, 988, 910, 772, and 695 cm^{-1} are the characteristic absorptions of ABS, and the assignments of the absorption peaks are presented in Table 5. The major pyrolytic gases are water (3600–3800 cm^{-1}), aromatic components (3075, 3028, 1946, 1820, 1629, 1494, 772, and 687 cm^{-1}), alkane (2937 and 1444 cm^{-1}), and butadiene (988 and 910 cm^{-1}) [26]. Upon addition of NPPh3/TPP to ABS, two additional peaks are observed: The peak at 1194 cm^{-1} can be assigned to the absorption of P=O, and the peak at 967 cm^{-1} is assigned to P–O stretching vibrations [27]. It dilutes the concentration of oxygen and fuel and then improves the flame retardancy of ABS.

Figure 9 shows that there is no significant difference between ABS and ABS/NPPh3/TPP-2 during the thermal

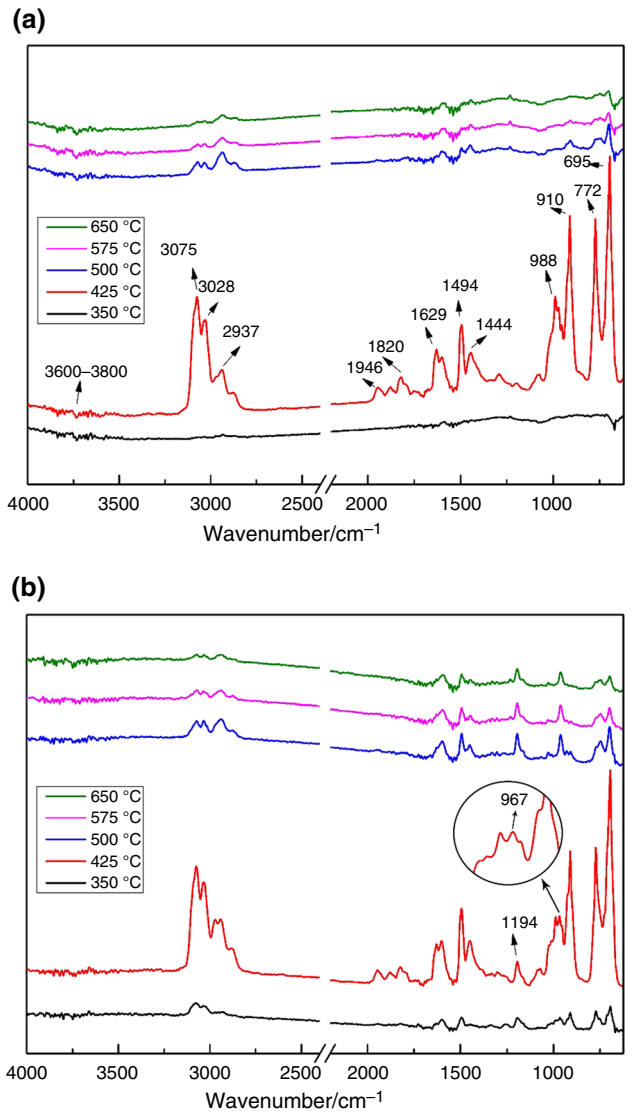

Fig. 8 FTIR spectra of pyrolysis products for **a** ABS and **b** ABS/NPPh3/TPP-2 at different temperatures

degradation process. In the temperature range of 280–500 °C, the peak strength of aromatic components and butadiene first increases with a rise in temperature. Then, the signal intensity declines gradually after the maximum degradation rate. It can be observed that ABS/NPPh3/TPP-2 starts to produce volatilized products at 350 °C, as shown in Fig. 8b, while ABS dose not decompose at the same temperature as shown in Fig. 8a. The incorporation of NPPh3/TPP stimulates the decomposition of ABS at low temperature. Figure 10 shows the FTIR absorbance curves of aromatic compounds (695 cm^{-1}) evolved from ABS and ABS/NPPh3/TPP-2 versus temperature. It can be seen that the absorbance intensity of the aromatic compounds for ABS/NPPh3/TPP-2 is lower than that of ABS after 400 °C, which means the rate of chain scission at main decomposition is lower.

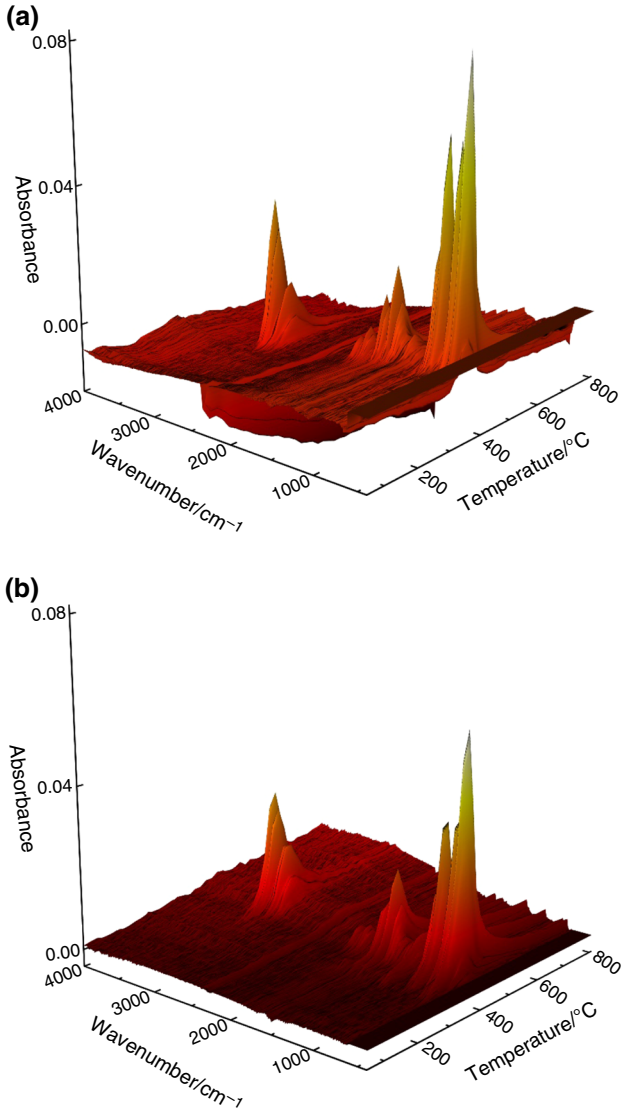

Fig. 9 3D TG-FTIR spectra of pyrolysis products for **a** ABS and **b** ABS/NPPh3/TPP-2

Table 5 Assignments of FTIR spectra of pyrolysis gases of ABS

Wave number/cm^{-1}	Assignment
3600–3800	νO–H
3075, 3028	νC_{Ar}–H
2937	νC–H (alkane)
1946, 1820	δC–H (aromatic ring)
1629, 1494	νC=C (aromatic ring)
1444	$\nu C–H_2$ (alkane)
988, 910	νC=C–H (butadiene)
772, 695	νC_{Ar}–H

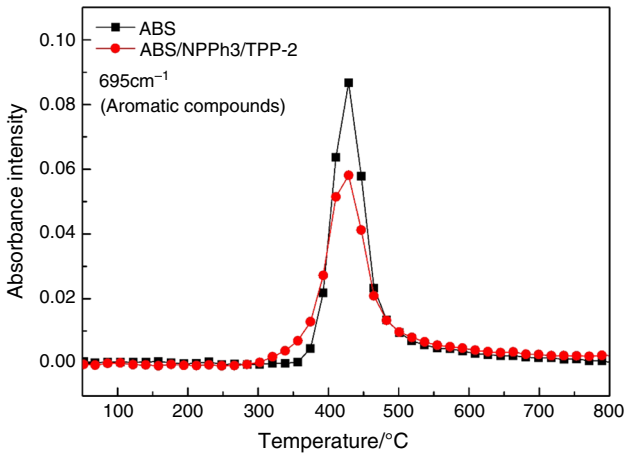

Fig. 10 FTIR absorbance curves of aromatic compounds evolved from ABS and ABS/NPPh3/TPP-2 versus temperature

Flame-retardant mechanism

From the above discussion, the flame-retardant mechanism of NPPh3/TPP in ABS is illustrated in Fig. 11. After the flame-retardant ABS is ignited, NPPh3/TPP induces ABS to decompose in advance and promotes to form a char layer which is rich with phosphorus and nitro group. This char is smooth and tight, can prevent heat and flammable gas transfer between the flame and substrate, and thus protects the underlying materials from further burning and pyrolysis. In gaseous phase, NPPh3/TPP releases some phosphorus-containing fragments with quenching effect and nonflammable gases with diluting effect. The phosphorus-containing free radicals can scavenge the H and OH in the flame, and the nonflammable gases such as CO_2 can dilute ignitable gases, thereby exerting a good flame inhibition

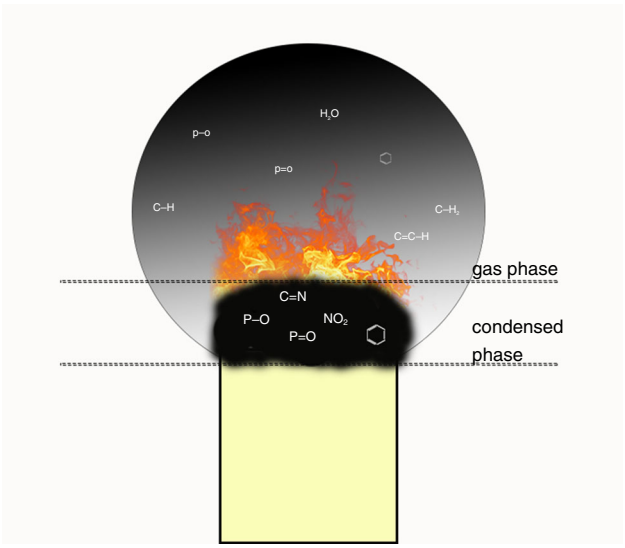

Fig. 11 Gas–condensed phase flame-retardant mechanism

effect. In other words, NPPh3/TPP shows a gas–condensed phase flame-retardant effect in ABS.

Conclusions

NPPh3/TPP flame-retardant system is applied in ABS. Compared with the ABS added NPPh3 and TPP alone in a same addition mass fraction, the LOI value of ABS/NPPh3/TPP increases. TG results under N_2 indicate that NPPh3/TPP has an influence on the degradation of ABS and improves the mass of char residue. Meanwhile, the TG results in air atmosphere for ABS/NPPh3/TPP demonstrate that NPPh3/TPP enhances the thermal stability of ABS, but does not improve the mass of char residue. This char residue is rich with phosphorus and nitro group, which could hinder the transfer of heat and combustible gas. Moreover, during combustion, ABS/NPPh3/TPP can release phosphorus-containing fragments into gaseous phase, which could scavenge the H and OH in the flame, thereby exerting a good flame-retardant effect. In consequence, ABS/NPPh3/TPP can be attributed to the synergic action of the condensed phase mechanism and gas barrier effects.

Acknowledgements We would like to thank the generous supports by the Experiment Center of Polymer Science and Engineering Academy, Sichuan University.

References

1. Hu X, Guo Y, Chen L, Wang X, Li L, Wang Y. A novel polymeric intumescent flame retardant: synthesis, thermal degradation mechanism and application in ABS copolymer. Polym Degrad Stab. 2012;97(9):1772–8.
2. Thanh Truc NT, Lee BK. Selective separation of ABS/PC containing BFRs from ABSs mixture of WEEE by developing hydrophilicity with ZnO coating under microwave treatment. J Hazard Mater. 2017;329:84–91.
3. Rojsatean J, Larpsuriyakul P, Prakymoramas N, Thanomjitr D, Kaewket S, Singsom T, Srinun D. Friction characteristics of self-lubricating ABS under different surface roughnesses and temperatures. Tribol Int. 2017;109:229–37.
4. Cantrell JT, Rohde S, Damiani D, Gurnani R, Disandro L, Anton J, Young A, Jerez A, Steinbach D, Kroese C. Experimental characterization of the mechanical properties of 3D-Printed ABS and polycarbonate parts[M]// Advancement of Optical Methods in Experimental Mechanics, Vol. 3. Springer International Publishing, 2017.
5. Liu Y, Yi J, Cai X. Effect of a novel intumescent retardant for ABS with synergist $Al(H_2PO_2)_3$. Polym Bull. 2011;67(2):361–74.
6. Jun W, Yi J, Cai X-F. Synergistic effect of a novel charring agent and ammonium polyphosphate on the flame retardancy of acrylonitrile butadiene styrene. J Appl Polym Sci. 2011;120(2):968–73.
7. Wang J, Cai X-F. Synergistic effect of a novel charring agent with ammonium polyphosphate on flame retardancy and thermal degradation of acrylonitrile-butadiene-styrene copolymer. Polym Int. 2012;61(5):703–10.
8. Yin H-Q, Yuan D, Cai X-F. The high efficiency two stage intumescent-contractive flame retardant on ABS. Polym Degrad Stab. 2013;98(1):288–96.
9. Min Y, Li P, Yin X-G, Ban D-M. Synthesis and characterization of an novel flame retardant based on phosphaphenanthrene for epoxy resin. Polym Bull. 2016;74(1):1–10.
10. Shih Y-F, Wang Y-T, Jeng R-J, Wei K-M. Expandable graphite systems for phosphorus-containing unsaturated polyesters. I. Enhanced thermal properties and flame retardancy. Polym Degrad Stab. 2004;86(2):339–48.
11. Matchimapiro T, Sornthummalee P, Pothisiri T, Rimdusit S. Impact behaviors and thermomechanical properties of TPP-filled polycarbonate/acrylonitrile-butadiene-styrene blends. J Metals. 2008;18:187–90.
12. Kim J, Lee K, Lee K, Bae J, Yang J, Hong S. Studies on the thermal stabilization enhancement of ABS; synergistic effect of triphenyl phosphate nanocomposite, epoxy resin, and silane coupling agent mixtures. Polym Degrad Stab. 2003;79(2):201–7.
13. Lee K, Kim J, Bae J, Yang J, Hong S, Kim HK. Studies on the thermal stabilization enhancement of ABS; synergistic effect by triphenyl phosphate and epoxy resin mixtures. Polymer. 2002;43(8):2249–53.
14. Chen L, Chen L, Guo H, Cai XF. The charring flame-retardant mechanism of TPP/TPPFR on ABS resin. Plastics. 2009;38(2):1–4.
15. Yang Y, Luo H, Cao X, Kong W, Cai X. Preparation and characterization of a water resistance flame retardant and its enhancement on charring–forming for polycarbonate. J Therm Anal Calorim. 2017;129(2):809–20.
16. Agrawal S, Narula AK. Synthesis and characterization of phosphorus containing aromatic poly(amide-imide)s copolymers for high temperature applications. Polym Bull. 2013;70(12):3241–60.
17. Bai CY, Tang XD, Chen XT, Zhang JH. Synthesis and characterization of bis(3-aminophenyl)phenyl phosphine oxide. Chem Reag. 2010;32(5):470–2.
18. Gao L-P, Wang D-Y, Wang Y-Z, Wang J-S, Yang B. A flame-retardant epoxy resin based on a reactive phosphorus-containing monomer of DODPP and its thermal and flame-retardant properties. Polym Degrad Stab. 2008;93(7):1308–15.
19. Ren Y-Y, Chen L, Zhang Z-Y, Wang X-L, Yang X-S, Kong X-J. L. yang, Synergistic effect of hydroquinone bis(di-2-methylphenyl phosphate) and novolac phenol in ABS composites. Polym Degrad Stab. 2014;109:285–92.
20. Yang S, Wang J, Huo S, Wang M, Wang J. Preparation and flame retardancy of a compounded epoxy resin system composed of phosphorus/nitrogen-containing active compounds. Polym Degrad Stab. 2015;121:398–406.
21. Zhang L, Wang Y, Liu Q, Cai X. Synergistic effects between silicon-containing flame retardant and DOPO on flame retardancy of epoxy resins. J Therm Anal Calorim. 2015;123(2):1343–50.
22. Zhang X, Zhong Y, Mao Z-P. The flame retardancy and thermal stability properties of poly (ethylene terephthalate)/hexakis (4-nitrophenoxy) cyclotriphosphazene systems. Polym Degrad Stab. 2012;97(8):1504–10.
23. Zhang L, Wang Y, Cai X. Effect of a novel polysiloxane-containing nitrogen on the thermal stability and flame retardancy of epoxy resins. J Therm Anal Calorim. 2016;124(2):791–8.
24. Zhao W, Liu J, Peng H, Liao J, Wang X. Synthesis of a novel PEPA-substituted polyphosphoramide with high char residues and its performance as an intumescent flame retardant for epoxy resins. Polym Degrad Stab. 2015;118:120–9.
25. Yang Y, Liu J, Cai X. Antagonistic flame retardancy between hexakis(4-nitrophenoxy) cyclotriphosphazene and potassium

diphenylsulfone sulfonate in the PC system. J Therm Anal Calorim. 2016;126(2):571–83.
26. Feng J, Carpanese C, Fina A. Thermal decomposition investigation of ABS containing Lewis-acid type metal salts. Polym Degrad Stab. 2016;129:319–27.
27. Yang S, Wang J, Huo S, Wang J, Tang Y. Synthesis of a phosphorus/nitrogen-containing compound based on maleimide and cyclotriphosphazene and its flame-retardant mechanism on epoxy resin. Polym Degrad Stab. 2016;126:9–16.